A Study on Carbon-Nanotube Local Oxidation Lithography Using an Atomic Force Microscope

Kitu Kumar, Onejae Sul, Stefan Strauf, Daniel S. Choi, *Member, IEEE*, Frank Fisher, Marehalli G. Prasad, and Eui-Hyeok Yang, *Senior Member, IEEE*

Abstract—In this paper, nanoscale anodic oxidation lithography using an atomic force microscope (AFM) is systematically studied on carbon nanotubes (CNTs). Trends between the produced feature size and the corresponding process parameters, such as applied voltage, water meniscus length, tip speed during oxidation (hold time), and humidity are observed. By methodically varying these process parameters, the appropriate working ranges have been found to create features of various sizes based on the oxidation of the CNT structure. We have obtained feature sizes down to 58 nm by setting oxidation time per pixel to 20 ms corresponding to a tip speed of 1.50 μm/s. Optimizing the tip speed during line scans was found to be critical in maintaining the presence of the water meniscus, which was often found to break above the tip speeds of 1 μm/s. In addition, a comparison of the results from employing this technique between CNT and graphene patterning is illustrated. Other factors affecting the reproducibility of the results are addressed in an endeavor to make the oxidization process more robust and repeatable.

Index Terms—Atomic force microscopy (AFM), carbon nanotube (CNT), graphene, lithography, nanotechnology.

I. BACKGROUND

THE ATOMIC force microscope (AFM) is typically used for imaging, but over the last two decades, it has also been used to fabricate devices on various materials using the principle of local anodic oxidation [1]–[8]. In a humid environment, where a water meniscus forms naturally between a conductive tip and substrate, an electric field applied to the tip will oxidize the substrate. Using the scanning capabilities of the AFM, various nanoscale features can be produced via oxidation of the material to form either volatile or nonvolatile oxides. Nonvolatile oxide deposition is widely used for application in nanoelectronics, where the oxide pattern electrostatically defines semicon-

ductor quantum dots [9], and for application in nanophotonics, where the local oxide can tune the mode frequency of photonic crystal nanocavities [10]. On the other hand, the ability to etch materials through the formation of volatile oxides opens possibilities for AFM tip-based nanolithography if the process parameters are understood and well controlled. For instance, if applied to graphitic materials, such as carbon nanotubes (CNTs) and graphene, tip-based patterning in the sub-100-nm range is a convenient desktop lithography alternative for the fabrication of novel quantum nanostructures that are required in emerging nanoelectronics applications [11]–[16]. While such structures can be fabricated using conventional e-beam lithography, AFM local oxidation, if fully implemented, is an attractive alternative with no resist processing steps or vacuum necessary. Recently, the AFM has been used to modify CNTs [17], [18]. While these studies have shown either oxidation lithography on CNTs or the effect of electric field on feature size, a study on the relationship between patterning parameters and features produced has not yet been performed. Therefore, the study described in this paper is to establish a set of empirical guidelines on the process parameters, such as voltage, meniscus length, tip speed, and relative humidity affecting feature size.

II. EXPERIMENTAL PROCEDURE

A Pacific Nanotechnology (NANO-I) AFM was modified with electrical connections between the tip mount and stage to the voltage source that came with the AFM (see Fig. 1). For all experiments, the substrate was kept grounded while the tip was negatively biased. Experiments with the substrate at positive voltage and a grounded tip showed similar results. Conductive diamond tips (Nanoscience Instr. NDCTCR1–2) were used for both imaging and oxidation procedures. The tips were imaged before initial use and after 1–2 months (180–200 h) of use with no discernable change in tip radius of curvature, which was determined to be 35 nm. The AFM scanning error was found to be $+/-$ 2.0 nm in the z-direction from roughness measurements and $+/-1.0$ nm in the x–y direction by comparing the measured dimensions of a standard calibration sample.

N-type [1 0 0] silicon wafers with the resistivity of 0.005-Ω cm (As doped) were purchased from Silicon Quest International and have been used as the substrates in these experiments. The cleaning procedure included acetone, methanol, and DI water baths followed by N_2 blow drying and prebaking at 170 °C for 5 min. A droplet of semiconducting single-walled CNTs (NanoIntegris) solution was dispersed, dried, and the remaining solution residue was removed using acetone and distilled, deionized water baths followed by soft baking at 100 °C.

K. Kumar, O. Sul, F. Fisher, M. G. Prasad, and E. H. Yang are with the Department of Mechanical Engineering, Stevens Institute of Technology, Hoboken, NJ 07030 USA (e-mail: kkumar@stevens.edu; Onejae.Sul@stevens.edu; Frank.Fisher@stevens.edu; mprasad@stevens.edu; eyang@stevens.edu).

S. Strauf is with the Department of Physics, Stevens Institute of Technology, Hoboken, NJ 07030 USA (e-mail: strauf@stevens.edu).

D. S. Choi is with the Department of Chemical and Materials Engineering, University of Idaho, Moscow, ID 83844 USA (e-mail: dchoi@uidaho.edu).
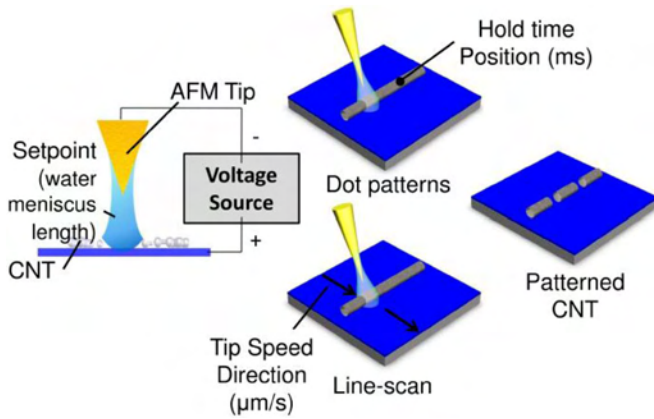
Fig. 1.   Schematic diagram of AFM oxidation lithography setup. An external voltage source is used to ground the CNT and negatively bias the AFM tip. The water meniscus, which naturally condenses around the tip, and CNT facilitates local oxidation of the CNT upon application of the electric field. The figures on the right illustrate the difference between dot patterns and line scans during oxidation. Dot patterns (top) involve holding the tip stationary at a point above the CNT (hold time position) and applying voltage to fabricate the patterns, while line scans (bottom) involve scanning the tip perpendicularly across the CNT at a constant tip speed and applying continuous voltage.

Suitable CNT samples for experimentation were identified by using either AFM or SEM imaging. Following the identification of the target CNT sample for study, the substrate was mounted on the AFM stage using copper tape and grounded to the built-in AFM voltage source. The supply voltage from this source was connected to the AFM cantilever scanner mount to facilitate biasing of the tip. Imaging of the CNTs before and after oxidation was conducted in the contact mode, while oxidation occurred in the noncontact mode. Parameters for AFM oxidation lithography that were varied include bias voltage, meniscus length (hereafter known as set point), and tip speed under high (>60%) and low (<30%) relative humidity conditions. The dependent parameter was the feature size (depth and width) of the oxidized sample, whose z-profile was determined using the Nanorule software by Pacific Nanotechnology. Patterns were created by either scanning the AFM tip at a constant speed and set point across the CNT while continuously applying a steady voltage (line scans), or by holding the tip over the CNT at a constant set point and applying steady voltage over a set hold time in milliseconds through a series of oxidation steps (dot patterns). In cases, where "dot" patterns were utilized, the tip speed was inferred from the applied AFM tip hold time per pixel.

III. EXPERIMENTAL RESULTS AND DISCUSSION ON LOCAL OXIDATION PARAMETERS

In the local anodic oxidation experiments, voltage was varied from −4 to −10 V, set point from 20 to 160 nm, and tip speed from 0.30 to 1.70 μm/s. In Fig. 2, line-scan experiments between set point, voltage, and feature size were conducted under high (>60%) and low (<30%) humidity conditions with a constant speed of 0.30 μm/s. Clear trends were observed between feature size and the three process parameters. The general trends can be explained by the tip–meniscus–substrate interaction. Raising or lowering the tip (increasing/decreasing the set point) has the ef-
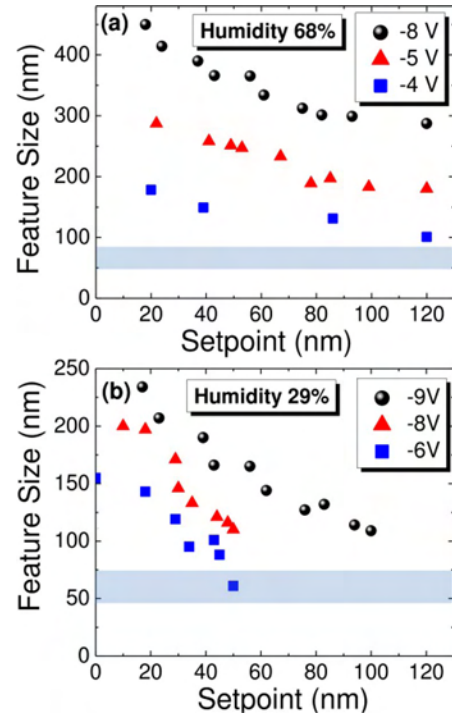

Fig. 2.   Feature-size dependence on set point and voltage under different humidity conditions. In both (a) high (>60%) and (b) low (<30%) humidity, a clear correlation is seen between voltage, set point, and feature size. Note that at set points beyond 120 nm, no oxidation occurs. This is attributable to water meniscus breakage during the oxidation scan and can be remedied by holding the tip stationary over the CNT.

fect of stretching or contracting the water meniscus and thereby decreasing or increasing its diameter, and therefore, reducing or increasing feature size. A change in voltage causes a change in the volume of oxidized carbon, such that a decreasing absolute voltage creates smaller features [4], [15]. At high humidity [see Fig. 2(a)], where the water meniscus was found to be stably bound to both tip and substrate up to a set point of 120 nm, the dominating factor controlling feature size was the voltage. An increase of 2 V from −8 to −6 V caused an average drop of feature size of around 200 nm for most data points. However, the smallest achieved features sizes of about 100 nm are still larger than the size of the AFM tip, which is highlighted by the blue shaded area in the figure, with the upper limit of 70 nm for the tip diameter and the lower limit of 35 nm for the tip radius.

Under low humidity conditions [see Fig. 2(b)], voltage was not the dominating factor, because a comparable 2 V increase resulted in an average drop in feature size of only 50–100 nm. In fact, reducing humidity from 68% to 29% in the range of tests studied here, keeping all other variables constant, had the effect of almost halving the feature sizes shown in Fig. 2(a). As the meniscus is caused by water condensation, lower humidity reduces meniscus diameter, thus, the smallest feature size achieved is slightly smaller than the AFM tip diameter and illustrates that humidity control is a very important parameter for high-resolution lithography.

Fig. 3 presents a comparison of feature-size dependence on tip speed between CNTs [see Fig. 3(a)] and exfoliated graphene
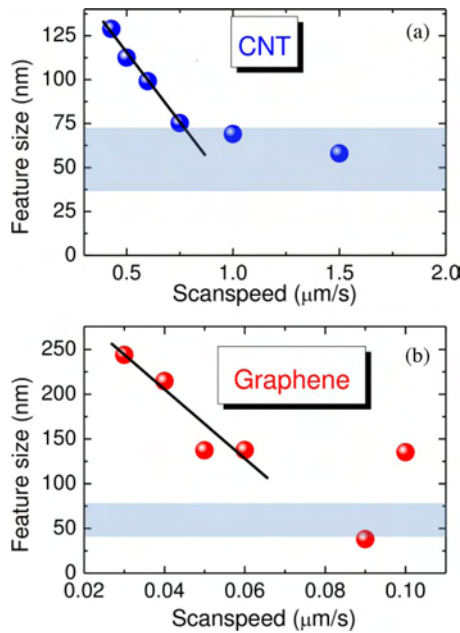
Fig. 3. Feature-width dependence of (a) CNT and (b) few layer graphene on AFM tip speed. In (a), as tip speed decreases and thus hold time per pixel increases, more carbon material is oxidized. Smaller feature sizes can be achieved for relatively fast tip speeds (1.00–1.50 μm/s) corresponding to short hold times. This trend is seen in (b) for slower tip speeds (0.03–0.06 μm/s) corresponding to longer hold times, but the feature-size dependence becomes inconsistent approaching faster tip speeds (above 0.06 μm/s.) This behavior is attributed to the hydrophobicity of graphene, especially under low humidity conditions.
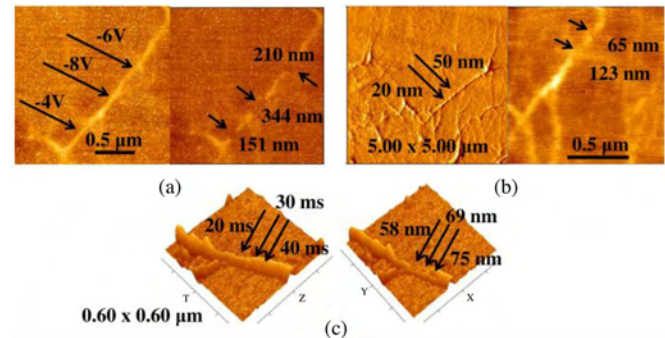

Fig. 4. AFM images of the local oxidation lithography process. (a) Effect of varying voltage on feature size (humidity is 66%, set point 45–50 nm, and tip speed 0.3 μm/s). (b) Varying set point (voltage −6 V, humidity 26%, and tip speed 0.3 μm/s). (c) Varying hold time (voltage −7.85 V, humidity 33%, and set point 45–50 nm). Drawing (c) dot patterns instead of (a)–(b) line scans can produce smaller feature sizes for the corresponding tip speeds during line scans.

flakes [see Fig. 3(b)] [19]. The exfoliated flakes for this study have about 7–15 graphene layers, as identified by their corresponding Raman signatures [20]. The results of the CNT patterning in Fig. 3(a) are taken from two sets of experiments under low humidity conditions (33%), low voltage (−7.85 V), and a 45–50-nm set point. The first three data points on the left are taken by line scans, and the three data points on the right at higher tip speed were recorded in the stationary "dot" patterning mode, in order to avoid meniscus breakage. The results from the graphene patterning are taken from the low humidity condition (30%), voltage of −10 V and a set point of 0 nm with the line-scan technique. In the case of CNTs, a clear relation between tip speed and feature size is seen, showing that the feature size decreases linearly with increasing tip speed in the range from 0.43 to 0.75 μm/s, resulting in the reduction of feature size from 129 to 75 nm. The longer the tip spends "drawing" each pixel, the more oxidation occurs, resulting in a larger feature size. The feature size tends to saturate when it approaches and passes the AFM tip diameter near at the upper limit of the blue region. Ultimately, it would be difficult to consistently write features smaller than the AFM tip radius, however, these experiments could be improved in the future using AFM tips with smaller radius of curvature.

In contrast, the general relation between tip speed and feature size is not as clear for the few layer graphene samples. The linear trend toward smaller feature sizes with faster tip speeds is maintained for until a tip speed of 0.06 μm/s, after which irregular behavior is observed, indicating the instability of the water meniscus. Additionally, at tip speeds above 0.10 μm/s

(smaller than 300 ms per pixel), no oxidation was observed on the substrate. This phenomenon and the inconsistency of the feature sizes patterned at high tip speeds (small hold times) is attributed to the hydrophobicity of the graphene layer and the resulting breakage of the water meniscus, which arises from water repulsion from the substrate, especially under the low humidity condition. Since feature hydrophobicity was not an issue for the CNT experiments, the base silicon substrate being less hydrophobic than graphene, faster tip speeds (smaller hold times) were employed for patterning.

In Fig. 4, several AFM scans detail various oxidation experiments on CNT bundles with an average height of 15–20 nm. The arrows in the left images of Fig. 4(a) and (b) shows the path of the AFM tip before oxidation, and Fig. 4(c) shows the position of the tip during each step. The results of CNT oxidation lithography are shown in the figures on the right, respectively. Fig. 4(a) shows the effect of voltage variation from −4 to −8 V in steps of 2 V on the size of the features patterned under high humidity. Doubling the voltage from −4 to −8 V results in more than a doubling of the feature size from 151 to 344 nm.

In Fig. 4(b), the oxidized areas on the CNTs are smaller in size than in Fig. 4(a). The feature size created by a 50-nm set point in Fig. 4(b) is 123 nm at −6 V, 26% humidity, and 0.30 μm/s tip speed. For the same voltage, set point, and tip speed in 66% humidity [see Fig. 4(a)], feature size nearly doubled to 210 nm. The 65-nm feature size in Fig. 4(b) is slightly less visible, and sub-20-nm feature sizes may be difficult to image with regular AFM, but can be easily imaged using electrical force microscopy [18]. The effect of increasing hold time per pixel (thereby increasing the virtual tip speed) is presented in Fig. 4(c). While this particular experiment was performed using dot patterns, the hold times 20, 30, and 40 ms, corresponding to tip speeds of 1.50, 1.00, and 0.75 μm/s, produced 58-, 69-, and 75-nm features, respectively. It is interesting to note that, although these results affirm the general trend of increasing tip speed resulting in decreasing feature size, these values could only be observed in dot patterns, not in line scans.

Line scans were primarily used for patterning to "capture" the CNT in the case of tip positioning errors. No oxidization was
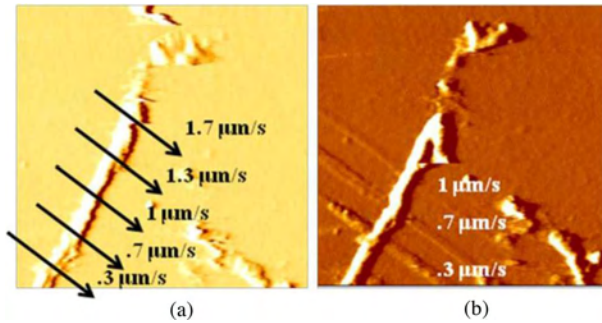
Fig. 5. Effect of tip speed on local oxidation nanolithography. Under low humidity conditions ($<25\%$ humidity), -10-V applied voltage, and 45–50-nm set point, one can see oxidation effects for tip speeds from 0.30 to 1.00 μm/s. At higher tip speed, no oxidization is observed, which is attributed to water meniscus breakage. High tip speeds (corresponding to short hold times) are required for small feature sizes.

typically observed over tip speeds of 1.00 μm/s, as illustrated in Fig. 5. This was caused most likely due to breakage of the water meniscus as the tip scanned across the various substrate features, in addition to the surface hydrophobicity influence of silicon. This problem might be overcome by drawing a series of dots for hold times corresponding to the faster tip speeds. Further, it is important to note that the water meniscus diameter is directly related to the radius of curvature of the AFM tip. The tip used in these experiments had a 35-nm radius of curvature, limiting feature size in these experiments to roughly double that value. Though the feature size can be reduced [see Fig. 4(b)] by stretching the water meniscus, the break threshold was found to be 120-nm set point for speeds greater than 1.00 μm/s during line scans. This is most probably due to meniscus breakage over variable morphology (nearby bundles, as shown in Fig. 5) as the tip scanned over the substrate. As aforementioned, the solution involves drawing dot patterns and applying voltage for shorter hold times. Here, set points greater than 120 nm may be achieved due to the inherent stability of the stationary patterning.

Overall, clear trends emerged during the oxidation experiments. It was found that feature size decreases if 1) voltage increases (becomes less negative), 2) meniscus length distance increases, 3) tip speed increases (corresponding to a decrease in hold time per pixel), and 4) humidity decreases, thus, creating higher resolution. Resolution of the patterning constraints caused by meniscus breakage during line scans at larger speeds and humidity control is currently being studied.

IV. CONCLUSION

This study on AFM-tip-based oxidation lithography performed on CNTs has determined clear relationships between the process parameters bias voltage, set point, tip speed, humidity, and the achievable feature size. A minimum feature size of 58 nm for CNTs (38 nm for graphene) was achieved in the range of process parameters considered here. The observed trends can be used to further reduce feature sizes for devices requiring CNT segments on the order of a few tens of nanometers. Further progress can be achieved by optimizing three key factors, which affect the local oxidation results: First, precise tip posi-

tioning is limited by the sensitivity of the piezoelectric stage controlling the tip mount, which is affected by temperature, humidity, and hysteresis. Second, the experiments described in this paper were conducted in an open-air environment. We anticipate that the incorporation of a controlled environmental cell is expected to reduce the possible effects of contaminants on the feature sizes. Finally, feature size is ultimately limited by the finite AFM-tip dimensions. In addition, since graphite and CNTs are both composed of sp^2–bonded carbon atoms, the observed trends have been found to be directly applicable to the controlled patterning of 2-D graphene and graphite layers, as reported elsewhere [19]. The presented empirical guidelines on the process parameters of local AFM-tip-based oxidation are useful to optimize the fabrication of graphitic nanostructures with applications in nanoelectronics and nanophotonics.

REFERENCES

[1] S. C. Minne, Ph. Flueckiger, H. T. Soh, and C. F. Quate, "Atomic force microscope lithography using amorphous silicon as a resist and advances in parallel operation," *J. Vac. Sci. Technol. B*, vol. 13, no. 3, pp. 1380–1385, May 1995.

[2] B. Irmer, M. Kehrle, H. Lorenz, and J. P. Kotthaus, "Fabrication of Ti/TiOx tunneling barriers by tapping mode atomic force microscopy induced local oxidation," *Appl. Phys. Lett.*, vol. 71, pp. 1733–1735, Sep. 1997.

[3] S. Myhra, "Tip-induced local anodic oxidation: Nanolithography and nanobiotechnology," *J. Nanobiotechnol.*, vol. 3, pp. 212–222, Dec. 2007.

[4] R. Garcia, R. V. Martinez, and J. Martinez, "Nano-chemistry and scanning probe nanolithographies," *Chem. Soc. Rev.*, vol. 35, pp. 29–38, Nov. 2005.

[5] S. Bae, C. Han, M. S. Kim, C. C. Chung, and H. Lee, "Atomic force microscope anodization lithography using pulsed bias voltage synchronized with resonance frequency of cantilever," *Nanotechnology*, vol. 16, pp. 2082–2085, Aug. 2005.

[6] R. Held, T. Heinzel, P. Studerus, and K. Ensslin, "Nanolithography by local anodic oxidation of metal films using an atomic force microscope," *Physica E*, vol. 2, pp. 748–752, Jul. 1998.

[7] P. Avouris, R. Martel, T. Hertel, and R. Sandstrom, "AFM tip induced and current induced local oxidation of silicon and metal," *J. Appl. Phys. A-Mater.*, vol. 66, pp. S659–S667, Mar. 1998.

[8] M. Tello and R. García, "Nano-oxidation of silicon surfaces: Comparison of noncontact and contact AFM methods," *Appl. Phys. Lett.*, vol. 79, pp. 424–426, Jul. 2001.

[9] M. Sigrist, A. Fuhrer, T. Ihn, K. Ensslin, D. C. Driscoll, and A. C. Gossard, "Multiple layer local oxidation for fabricating semiconductor nanostructures," *Appl. Phys. Lett.*, vol. 85, pp. 3558–3560, Oct. 2004.

[10] K. Hennessy, C. Högerle, E. Hu, A. Badolato, and A. Imamoğlu, "Tuning photonic nanocavities by atomic force microscope nano-oxidation," *Appl. Phys. Lett.*, vol. 89, pp. 041118-1–041118-3, Jul. 2006.

[11] G. A. Steele, G. Götz, and L. P. Kouwenhoven, "Tunable few-electrodes double quantum dots and Klein tunnelling in ultra-clean carbon nanotubes," *Nature Nanotech.*, vol. 4, pp. 363–367, Jun. 2009.

[12] S. Sapmaz, P. Jarillo-Herrero, Y. M. Blanter, and H. S. J. van der Zant, "Coupling between electronic transport and longitudinal phonons in suspended nanotubes," *New J. Phys.*, vol. 7, pp. 243-1–241-10, Nov. 2005.

[13] S. Moriyama, T. Fuse, M. Suzuki, Y. Aoyagi, and K. Ishibashi, "Four-electron shell structures and an interacting two-electron system in carbon-nanotube quantum dots," *Phys. Rev. Lett.*, vol. 94, pp. 186806-1–186806-4, May 2005.

[14] K. Ishibashi, S. Moriyama, D. Tsuya, T. Fuse, and M. Suzuki, "Quantum-dot nanodevices with carbon nanotubes," *J. Vac. Sci. Technol. A*, vol. 24, pp. 1349–1355, Jun. 2006.

[15] A. Javey, J. Guo, Q. Wang, M. Lundstrom, and H. Dai, "Ballistic carbon nanotube field-effect transistors," *Nature*, vol. 424, pp. 654–657, Aug. 2003.

[16] W. Liang, M. Bockrath, D. Bozovic, J. H. Hafner, M. Tinkham, and H. Park, "Fabry-Perot interference in a nanotube electron waveguide," *Nature*, vol. 411, pp. 665–669, Jun. 2001.

[17] D. H. Kim and J. Y. Koo, "Cutting of multiwalled carbon nanotubes by a negative voltage tip of an atomic force microscope: A possible mechanism," *Phys. Rev. B*, vol. 68, pp. 113406-1–113406-3, Sep. 2003.

[18] J. Y. Park, Y. Yaish, M. Brink, S. Rosenblatt, and P. L. McEuen, "Electrical cutting and nicking of carbon nanotubes using an atomic force microscope," *Appl. Phys. Lett.*, vol. 80, pp. 4446–4448, Jun. 2002.

[19] K. Kumar, S. Strauf, and E. H. Yang, "A study on graphite local oxidation lithography using an atomic force microscope," *Nanosci. Nanotechnol. Lett.*, vol. 2, no. 2, pp. 185–188, 2010.

[20] M. Begliarbekov, J. Sul, S. Kalliakos, E. H. Yang, and S. Strauf, "Determination of edge purity in bilayer graphene using μ-Raman spectroscopy," *Appl. Phys. Lett.*, vol. 97, 031908, Jul. 2010.

Kitu Kumar received the B.E. degree from the Mechanical Engineering Department, Stevens Institute of Technology, Hoboken NJ, in 2006.

In 2008, she joined E.H. Yang.s group as a Research Assistant. She is the author of more than ten presentations and publications. She holds a patent on nanolithography. Her current research interests include fabrication of graphene and carbon nanotube devices for nanoelectronics and energy storage applications.

Dr. Kumar is the recipient of an NSF GK-12 Graduate Teaching Fellowship in 2008 and the Robert Crooks Stanley Fellowship in 2010.

Onejae Sul received the B.S. degree from Korea University, Seoul, Korea, in 1996, and the M.S. and Ph.D. degrees from the University of North Carolina, Chapel Hill, in 2004 and 2006, respectively.

In 2007, he joined Prof. E.-H. Yang's group as a Postdoctoral Scholar, Mechanical Engineering Department, Stevens Institute of Technology, Hoboken, NJ, where he is currently a Research Scientist, and also member of the Process and Technique Committee, Micro Device Laboratory. He is the author of more than 20 presentations and publications. His research interests include device fabrication and novel phenomena investigation in the nanoscience and technology, such as development of nanoactuators, and nanoelectrooptic phenomena of carbon nanotube and graphene.

Stefan Strauf received the M.S. and Ph.D. degrees from the Physics Department, Bremen University, Bremen, Germany, in 1998 and 2001, respectively.

He was at the Institute of Solid-State Physics, Bremen, where he was engaged on entangled photons from CdSe quantum dots. In 2003, he joined UC Santa Barbara as a Postdoctoral Researcher. In the Fall of 2006, he joined the Department of Physics and Engineering Physics, Stevens Institute of Technology as an Assistant Professor. He is the author or coauthor of more than 50 papers, including 12 letter journal papers. His current research interests include nanophotonics and nanolelectronics involving semiconductor quantum dots, carbon nanotubes, and graphene.

Dr. Strauf has led a collaborative research effort addressing projects in photonic crystal nanolasers and single photon sources supported by National Science Foundation and DARPA. He was the recipient of a Max-Kade Foundation Fellowship in 2003 and the Davis Memorial Award for Research Excellence in 2008.

Daniel S. Choi (M'99) received the Ph.D. degree in electrical engineering of University of California, Los Angeles.

He worked for three years at Electronics and Photonics Laboratory, Aerospace Corporation, developing high-resolution focused ion beam and electron beam lithography. In 1999, he joined Jet Propulsion Laboratory, NASA as a member of engineering staff, where he worked on development of microseismometers and narrow-band MEMS IR gas sensors for space applications. He was also involved in research on gel-free molecular sieve based on carbon nanotube vertical arrays for DNA sequencing and high-quality-factor (Q) nanomechanical resonators with carbon nanotubes. He is currently an Associate Professor in the Department of Materials Science and Engineering, University of Idaho, Moscow, ID, where he is leading projects related to nanotechnology: 1) nanofluidic size exclusion chromatograph for lab-on-a-chip applications; 2) novel nanomanipulation with nanotubes for bioapplications; and 3) nanowire-based energy applications (solar cells and Li-ion batteries).

Frank Fisher received the B.S. degrees in mechanical engineering and applied mathematics from the University of Pittsburgh, Pittsburgh, PA, in 1995, and the M.S. degrees in mechanical engineering and learning sciences (School of Education and Social Policy) in 1998 and 2000, respectively, and the Ph.D. degree in mechanical engineering in 2002, all from Northwestern University, Evanston, IL.

He is currently an Associate Professor in the Department of Mechanical Engineering and the Co-Director of the Nanotechnology Graduate Program (www.stevens.edu/nano), Stevens Institute of Technology, Hoboken, NJ. His research interests include characterization of multifunctional nanoreinforced polymer systems, multiscale modeling of nanocomposites and materials, NEMS/MEMS sensors and devices, and vibration energy harvesting/scavenging.

Prof. Fisher is the recipient of the National Science Foundation's CAREER Award, the American Society of Engineering Education Mechanics Division Ferdinand P. Beer, and E. Russell Johnson Jr. Outstanding New Educator Award, the 2009 Outstanding Teacher Award from the Stevens Alumni Association, and the 2006 Harvey N. Davis Distinguished Teaching Assistant Professor Award from Stevens. He is currently the Chair of the American Society of Mechanical Engineering Materials Division Polymers Technical Committee.

Marehalli G. Prasad received the B.E. degree from the University College of Engineering, Bangalore, India, in 1971, the M.S. degree from the Indian Institute of Technology, Madras, India, in 1974, and the Ph.D. degree from Purdue University, West Lafayette, IN, in 1980, respectively, all in mechanical engineering.

He is currently a Professor and the Director of Noise and Vibration Control Laboratory, Department of Mechanical Engineering, Stevens Institute of Technology, Hoboken, NJ. His research interests include acoustics, vibration, noise control, and energy harvesting.

Prof. Prasad was the recipient of two research awards for his papers. He has worked as Noise Control Expert for United Nations projects in Romania and India. He is a Fellow of the American Society of Mechanical Engineers, the Acoustical Society of America, the Acoustical Society of India, and a Board Certified Member of the Institute of Noise Control Engineering.

Eui-Hyeok Yang (SM'05) received the B.S., M.S., and Ph.D. degrees from Ajou University, Suwon, Korea.

In 1996, he joined Fujita microelectromechanical systems (MEMS) research group, Institute of Industrial Science, University of Tokyo, Japan, as a Postdoctoral Scholar. He was also with Electronics and Telecommunications Research Institute (ETRI). In 1998, he joined the Jet Propulsion Laboratory (JPL), NASA, where he initiated and led the development of MEMS actuator technology thrust. He was a Senior Member of the Engineering Staff and Task Manager at JPL. He was a Technical Monitor for a NASA SBIR project. He is currently an Associate Professor at Mechanical Engineering Department, Stevens Institute of Technology, Hoboken, NJ, where he is also the Director of Multi-User Micro Device Laboratory (MDL). He holds ten patents issued or pending. His current research interests include 3-D carbon nanotube and graphene structures, graphene-based electronic, and sensing devices, as well as active nanosurfaces based on smart polymers and nanoactuator arrays.

Dr. Yang is a recipient of a research fellowship from the Japan Society for the Promotion of Science from 1996 to 1998. He is also the recipient of a number of awards, including NASA Inventions and Contributions Board Space Act Awards, Level B and C Awards, and Class 1 NASA Tech Brief Awards (over 30 awards). In recognition of his excellence in advancing the use of MEMS-based actuators for NASA's space applications, he received the prestigious Lew Allen Award for Excellence at JPL in 2003. He was a Research Adviser for National Research Council in piezoelectric microactuators for active-mirror technologies until 2006. He has been the Principal Investigator (PI)/Co-PI on grants and contracts from Air Force Office of Scientific Research, National Science Foundation, NASA, and the U.S. Army Armament Research, Development and Engineering Center. He is an Associate Editor of several journals, including *IEEE Sensors Journal*. In addition, he has been actively involved in the ASME MEMS Division as a member of Executive Committee. He is currently a Track Chair of Micro- and Nanomaterials, Devices and Systems Track of the ASME International Mechanical Engineering Congress and Exposition.